S. Kottuparambil, S. Agusti / Chemosphere 259 (2020) 127487

Cell-by-cell estimation of PAH sorption and subsequent toxicity in marine phytoplankton

Sreejith Kottuparambil[1]*, Susana Agusti[1]

Abstract

Polycyclic Aromatic Hydrocarbons (PAHs) have elicited increasing concern due to their ubiquitous occurrence in coastal marine environments and resultant toxicity in organisms. Due to their lipophilic nature, PAHs tend to accumulate in phytoplankton cells and thus subsequently transfer to other compartments of the marine ecosystem. The intrinsic fluorescence properties of PAHs in the ultraviolet (UV)/blue spectral range have recently been exploited to investigate their uptake modes, localization, and aggregation in various biological tissues. Here, we quantitatively evaluate the sorption of two model PAHs (phenanthrene and pyrene) in three marine phytoplankton species (*Chaetoceros tenuissimus*, *Thalassiosira* sp. and *Proteomonas* sp.) using a combined approach of UV excitation flow cytometry and fluorescence microscopy. Over a 48-h exposure to a gradient of PAHs, *Thalassiosira* sp. showed the highest proportion of PAH-sorbed cells (29% and 97% of total abundance for phenanthrene and pyrene, respectively), which may be attributed to its relatively high total lipid content (33.87 percent dry weight). Moreover, cell-specific pulse amplitude modulation (PAM) microscope fluorometry revealed that PAH sorption significantly reduced the photosynthetic quantum efficiency (F_v/F_m) of individual phytoplankton cells. We describe a rapid and precise hybrid method for the detection of sorption of PAHs on phytoplankton cells. Our results emphasize the ecologically relevant sub-lethal effects of PAHs in phytoplankton at the cellular level, even at concentrations where no growth inhibition was apparent. This work is the first study to address the cell-specific impacts of fluorescent toxicants in a more relevant toxicant-sorbed subpopulation; these cell-specific impacts have to date been unidentified in traditional population-based phytoplankton toxicity assays.

Keywords: PAHs, phytoplankton, fluorescence, adsorption, flow cytometry, F_v/F_m

1. Introduction

Contamination of the oceanic environment by petroleum hydrocarbons is an urgent concern for marine systems worldwide and their ecological health. With industrial expansion and widespread consumption of fossil fuels, there has been a subsequent increase in anthropic inputs of polycyclic aromatic hydrocarbons (PAHs). PAHs are the most acutely toxic components of petroleum crude oil, and are among the most ubiquitous and intensely investigated marine pollutants over recent decades (González-Gaya et al., 2016). PAHs are lipophilic and, therefore, exhibit high affinity for the cell membrane lipoproteins of planktonic organisms, subsequently entering the food chain via strong bioaccumulation, mobility, and environmental persistence. Because of their ubiquity, toxicity, and potential for human exposure, PAHs are rated as priority pollutants by several regulatory agencies, including the US Environmental Protection Agency (EPA), the European Union, and the Agency for Toxic Substances and Disease Registry (ATSDR).

A significant proportion of PAHs in the ocean is associated with suspended particles. For instance, suspended particles sampled along the coast of Xiamen Island, China (Ya et al., 2014) showed enrichment factors between 0.43 and 3.56, and from 5 to 145 in Southern Chesapeake Bay (Liu & Dickhut, 1997). Recent studies have reported the concentration of total PAHs in several oceanic regions, such as 179 ng l^{-1} in the Gulf of Trieste in the northern Adriatic Sea (Penko & Bajt, 2019), 9.36 ng l^{-1} in the southeastern Japan Sea (Hayakawa, 2018) and 43 ng l^{-1} in the Strait of Sicily, and the central Mediterranean Sea (Vecchiato et al., 2018). Even higher values have been reported for coastal waters, ranging from 50 to 1000 ng L^{1} in Chesapeake Bay (Liu & Dickhut, 1997), 4228 to 29325 ng l^{-1} for Daya Bay (Zhou & Maskaoui, 2003) and up to 459 ng L^{-1} in the Saronikos Gulf (Valavanidis et al., 2008). Furthermore, several studies have described the extent of PAH contamination in marine biota all over the globe (Ferrante et al., 2018; Ke et al., 2017; Ramalhosa et al., 2012). However,

the number of such studies are limited because the methods for detection of PAHs in biological tissues are considerably labor-intensive and time- and cost-ineffective. Moreover, PAH detection conventionally relies on destructive methods such as high-performance liquid chromatography (HPLC) and gas chromatography (GC), where the selection of an apt calibration is crucial (Cyr et al., 2019).

PAHs, due to their aromatic structure, are highly fluorescent under low UV (200–400 nm) excitation. Thus, PAHs in environmental samples can be detected by their characteristic fluorescence emission in the blue-green region (400–500 nm) of the spectrum using HPLC and fluorescence spectroscopy (Poster et al., 2006). Several analytical studies have focused on the specific PAH fluorescence signal to detect and quantify them in water, sediments (Cyr et al., 2019; Rodriguez & Sanz, 2000; Sarrazin et al., 2006), and biological samples (Alves et al., 2017; Augusto et al., 2015; Pena et al., 2015; Zhang et al., 2010). Likewise, fluorescence microscopy has demonstrated the uptake and accumulation of toxic PAHs in planktonic organisms (Subashchandrabose et al., 2014). However, the excessive time and labor requirements of these methods have limited the widespread applicability of this method to visualize PAH sorption in a larger number of target cells, such as in a phytoplankton population.

In the marine environment, phytoplankton constitute the most fundamental component of ecosystems and the energy cycle. Phytoplankton are particularly vulnerable to pollutants, and exposure to toxic PAHs is among the most severe threats to their abundance and physiology, especially in coastal habitats. Adverse effects of PAHs in marine phytoplankton include photosynthetic inhibition (Othman et al., 2012), DNA damage (Cerezo & Agustí, 2015), reduced gene expression (Bopp & Lettieri, 2007), oxidative stress (Vega-López et al., 2013), influence on abundance and distribution (Echeveste et al., 2016; Kottuparambil & Agusti, 2018), and trophic transfer to consumers (Froehner et al., 2011).

Flow cytometry is a well-established tool used in marine science to investigate the structure and distribution of phytoplankton communities in the marine environment (Anglès et al., 2015; Gérikas Ribeiro et al., 2018). A large number of observations in flow cytometry provide reliable ecological data through its high accuracy in counting and the high degree of precision (Rutten et al., 2005). In recent decades, the introduction of flow cytometry to monitor microalgal ecotoxicology has led to multispecies/multiparameter test methods, which have enabled the development of more environmentally relevant aquatic and sediment toxicity tests (Franklin et al., 2004; Stauber et al., 2002). Flow cytometry also permits a comprehensive analysis of the effects of PAHs on marine phytoplankton (Croxton et al., 2015). (Cerezo et al., 2017) described a relatively simple flow cytometry method based on autofluorescence to identify and quantify the proportion of phytoplankton cells with accumulated PAHs on their surfaces. The authors devised UV (355−405 nm) excitation flow cytometry coupled with a standard 488 nm laser to identify the characteristic fluorescence signal from PAHs (360−430 nm) adsorbed on individual algal cells. A significant highlight of their method was the robust cell-by-cell analysis, whose relevance and accuracy are superior to traditional population-based methods. Although high-throughput flow cytometric measurements of multiple parameters of individual cells is possible, conventional microscopic methods are still necessary for detailed quantification studies in microalgae. Therefore, combining flow cytometry with fluorescence microscopy presents a promising methodology to visualize toxic PAHs inside algal cells.

The goal of the present study is to improve the methodology to identify PAH sorption in marine phytoplankton, through a combination of flow cytometry and microscopy PAM fluorometric techniques. We report significant results with three phytoplankton species isolated from the Red Sea. PAH contamination is a prevailing environmental issue in the Red Sea, and significant level of total PAHs has been recently reported in water (298.32 ng l^{-1})

and sediment (2599 ng g^{-1} dry wt.) samples of the Red Sea (Al-Mur, 2019; Qari & Hassan, 2017). The Red Sea receives significant levels of hydrocarbon contamination through the discharge of industrial and sewage wastewater and urban emissions. Phenanthrene and pyrene are the most widespread and abundant PAHs in the Red Sea environment (Al-Mur, 2019). This study outlines an advancement in the methods to monitor and analyze the toxic impacts of PAHs in key marine phytoplankton taxa.

2. Materials and Methods

2.1 Phytoplankton cultures

Two bacillariophytes (*Chaetoceros tenuissimus* and *Thalassiosira* sp.) and one cryptophyte (*Proteomonas* sp.) species were isolated at the Qita Al Kirsh reef station (22.43 ^{o}N, 38.99 ^{o}E) and the coastal pelagic station (22.31^{o}N, 38.99^{o}E) in the Red Sea, respectively, after filtration through a 45 µm filter. Approximately ten clonal cultures were established using the precise single-cell isolation technique under a microscope (Axioscope A1, Carl Zeiss, Oberkochen, Germany) in filtered, sterilized, and enriched (f/2 and silicate for diatoms) seawater collected at the pelagic station. These isolates were cultivated as unialgal batch cultures at 24 ºC under 150 µmol photons m^{-2} s^{-1}, with a 12:12 light/dark cycle. Cells under the exponential growth phase were used for the experiments.

2.2 Test Chemicals

Phenanthrene ($C_{14}H_{10}$, CAS No. 85-01-8) and pyrene ($C_{16}H_{10}$, CAS No. 129-00-0) stocks were obtained as standard solutions in Methanol from Sigma Aldrich (Sigma Aldrich, Germany), with respective concentrations of 5000 and 1000 mg L^{-1}. Working stocks for each PAH (5, 50, 100, 300, 600, and 900 mg L^{-1}) were prepared by dilution in HPLC-grade

methanol, under controlled conditions to prevent the loss of solvent by evaporation. Stocks were tightly capped and stored in the dark at 4 ºC.

2.3 Experimental setup

50 µl of the individual PAH stocks were pipetted into acid pre-cleaned 125 ml Erlenmeyer flasks and kept inside a fume hood for 10 minutes to allow the solvent to evaporate in air at room temperature. Triplicate flasks were prepared for six PAH dosages (5, 50, 100, 300, 600, and 900 µg L^{-1}) and an untreated control. 50 ml of the algal culture was subsequently dispensed to each flask and swirled gently to ensure complete dissolution of the PAHs. The initial abundance was 10^4 and 10^5 cells ml^{-1} for bacillariophytes and cryptophyte, respectively. The flasks were tightly capped and incubated at 24 ^oC in a temperature-controlled incubator (Percival Scientific Inc., USA) with a 12:12 h light:dark cycle under 150 µmol photons m^{-2} s^{-1}. The flasks were occasionally swirled to facilitate uniform exposure to the PAH toxicant. After 48-h incubation, the samples were subjected to flow cytometric and microscopic measurements. In addition, a series of flow cytometry measurements were conducted to investigate the temporal changes in the sorption of pyrene in *Thalassiosira* sp. over a 96 h period, including sampling after 6, 24, 48, 62, and 96 hours.

2.4 Flow cytometry measurements

Absolute counts of phytoplankton cells and the proportion of cells with and without PAH sorption were estimated using a high performance, bench-top flow cytometer specially configured with a UV laser (375 nm) and a 488-nm blue solid-state laser (CyFlow Space, Sysmex Partec GmbH, Germany). Data were acquired by triggering chlorophyll fluorescence (FL3, 675 nm) in log mode, and the populations were enumerated following standard protocols (Franklin et al., 2001) based on the characteristic signals in the cytogram of FL3

versus side scatter (SSC). Dead cells and debris were excluded from enumeration by gating on an SSC/FL3 dot plot.

The characteristic PAH fluorescence signals were detected on the histogram of FL4 (excitation 375 nm; emission band-pass 455−40), which corresponded to the signals in the blue region. Firstly, the mean intensity of blue fluorescence was determined for the untreated control population. The corresponding subset of the population was gated and assumed to be the control cells with no PAHs sorbed in them. An increase in the mean blue fluorescence value was subsequently measured for the PAH-exposed cells (Cerezo et al., 2017), which was estimated in a separate gate next to the control gate. All counts were measured as cells ml^{-1}.

2.5 Fluorescence microscopy and microscopy PAM measurements

PAH sorption on the individual phytoplankton cells was visually analyzed using an Axioscope A1 epifluorescence microscope (Carl Zeiss, Oberkochen, Germany) equipped with a UV LED module (365 nm; Carl Zeiss, Oberkochen, Germany). A sample from each flask was mounted on a clean Marienfeld microscope slide (Paul Marienfeld GmbH & Co., Germany) and observed under the microscope under epifluorescence mode (Filter set 02, G 365, FT 395, LP 420, Carl Zeiss, Oberkochen, Germany). Cells with PAH sorption were distinguished by the characteristic blue fluorescing PAH blotches, while cells without PAH sorption appeared in red. At least 300 cells were manually counted and the proportion of PAH-sorbed cells was calculated. Images of phytoplankton cells were taken and processed using Zen pro software (Carl Zeiss, Oberkochen, Germany). The manual microscopic estimation of PAH sorption was numerically compared with the flow cytometry counts.

Simultaneously, the photosynthetic efficiency of PAH-sorbed and normal cells were distinctly estimated using a Microscopy Pulse-Amplitude-Modulated fluorometer (M-PAM, Heinz Walz GmbH, Effeltrich, Germany) connected to the microscope. Before switching to

the PAM-mode, the cells to be measured were focused under normal light-view mode at 400x magnification. Care was taken to expose the cells to the lowest possible irradiance to avoid any potential photoinhibitory effects of the transmitted light. The cells were detected very quickly for their fluorescence signature under epifluorescence mode, avoiding the photobleaching effects of the applied UV irradiation. The microscope was subsequently switched to the M-PAM mode, and the reflector turret was rotated to activate the blue excitation source. After a few minutes of dark adaptation, a fluorescence excitation was provided by a saturating pulse of the 470-nm LED module with an appropriate reflector module (Excitation: 450−490 nm, Emission: LP 515 nm; Carl Zeiss, Oberkochen, Germany), and the red fluorescence from the sample, collected by the objective lens, was directed with high efficiency towards a photomultiplier detector. The pre-amplified signal from the detector was subsequently processed in the PAM control unit, operated by the data acquisition and analysis software, WinControl V3.29 (Heinz Walz GmbH, Effeltrich, Germany). The maximum quantum efficiency of photosystem II (PS II) was derived as $F_v/F_m = (F_m–F_o)/F_m$, where F_m is the maximum fluorescence yield and F_o is the static minimum fluorescence yield of the dark-adapted cells (Schreiber et al., 1995). A detailed description of the M-PAM has been provided by Goh et al. (Goh et al., 1999).

2.6 Lipid extraction and analysis

The lipid contents in the phytoplankton cells were estimated gravimetrically following the standard procedure devised by Folch et al. (Folch et al., 1957). Cells from triplicated cultures at exponential growth phase were harvested by centrifugation at 7000 × *g*, 15 ^{o}C for 15 minutes (Avanti J-26 XP Centrifuge, Beckman Coulter, Krefeld, Germany). The pellets were subsequently lyophilized (Christ. Alpha 1-2 LD plus, Osterode am Harz, Germany) and stored at −80°C until analysis. For lipid estimation, ~50 mg of dry biomass was weighed and homogenized in a 2:1 chloroform:methanol (v/v) mixture with 0.01% BHT for 5 min by

sonication. The chloroform fractions of the recovered lipids were separated by centrifugation and gravimetrically estimated once the solvent was completely evaporated under a stream of N_2. The total lipid extract was subjected to alkaline transesterification. The lipid content, expressed as the percentage of total dry weight (DW), was calculated by the following formula:

$$X\ (\%) = \frac{X(T)}{Y} \times 100 \qquad (1)$$

where X (%) is the lipid percentage, X(T) is the total lipid, and Y is total biomass dry weight.

2.7 Data Analysis

All values presented here are the means ± 95% confidence intervals. All results were analyzed by ANOVA (n = 3; at $p = 0.05$) and Tukey test at 95% confidence to detect significant differences among the treatments using JMP software (JMP® Pro version 13.1, SAS Institute, USA).

The percentage of PAH-sorbed cells was calculated as the number of cells showing blue emission relative to the total number of cells in the population,

$$\frac{PAHs{-}sorbed\ cells}{Total\ cells} \times\ 100 \qquad (2)$$

The lethal concentration of PAHs, at which 10% of the decline in population abundance occurred (LC_{10}), was obtained by linear regression, applying the following equation (Echeveste et al., 2016) using JMP software.

$$LC_{10} = \ln 0.9/\Omega \qquad (3)$$

where Ω is the slope of the relationship between the ln of the cell abundance at the end of the experiment versus the PAH concentrations tested.

The EC_{10} values for F_v/F_m and their respective confidence intervals (95%) were calculated using a log-normal model in the Excel macro REGTOX (version 7.0.4, (Vindimian, 2010).

Nonparametric Spearman's rank correlation analysis was performed using JMP software to show the relationship between PAHs sorption by the tested phytoplankton and the respective lipid levels. Correlations (Spearman's correlation coefficient (ρ)) were considered statistically significant when $p < 0.05$.

3. Results

3.1 Estimation of PAH sorption by UV excitation flow cytometry

We detected the sorption of PAHs onto the phytoplankton cell surface by measuring the significant increase in the mean intensity of UV-induced blue fluorescence signals. However, the pattern and intensity of PAH fluorescence varied between the tested chemicals and the algal species. Pyrene showed consistently higher levels of sorption than phenanthrene in all the phytoplankton tested. *C. tenuissimus* showed distinct PAH fluorescence in all treated suspensions above 50 μg L^{-1} PAHs, scoring up to 5% and 35% of the total population, at 900 μg L^{-1} of phenanthrene and pyrene, respectively (**Fig. 1**). While phenanthrene caused no reduction in cellular growth of *C. tenuissimus*, the higher sorption of pyrene was accompanied by a significant (ANOVA, $df = 6$, $F = 10.48$, $p = 0.0002$) decay in abundance, with a 48-h LC_{10} value of 253.52 ± 101 μg L^{-1} (**Table 1**). Both phenanthrene and pyrene exhibited relatively higher affinity to *Thalassiosira* sp., resulting in respective > 20% and > 90% cells with PAH fluorescence at concentrations above 300 μg L^{-1} (**Fig. 2**), with 40% of cells showing pyrene sorption at 50 μg L^{-1} (**Fig. 2**). Moreover, the effect of PAHs on the final abundance was insignificant (ANOVA, $df = 6$, $F = 1.98$, $p = 0.14$) for phenanthrene and significant (ANOVA, $df = 6$, $F = 8.26$, $p = 0.0006$), albeit minimal, for pyrene. In *Proteomonas* sp., phenanthrene sorption was detected in negligible levels up to 1%, while pyrene sorption ranged from 10% at 50 μg L^{-1} to 39% at the highest two dosages (**Fig. 3**). Conversely to diatoms, phenanthrene exerted more significant inhibitory effects than pyrene to the abundance of *Proteomonas* sp. (ANOVA, $df = 6$, $F = 5.48$, $p = 0.004$).

Taxon	Lipid content (% DW)	Test PAH	PAH sorption$_{max}$ (%)	LC_{10} (µg L^{-1})	EC_{10} for F_v/F_m (µg L^{-1})
C. tenuissimus	7.22 ± 0.7	Phenanthrene	5.28 ± 0.06	ND	ND
		Pyrene	34.75 ± 1.33	253.52 ± 52	42.44 ± 20.84
Thalassiosira sp.	33.87 ± 0.6	Phenanthrene	28.69 ± 1.78	ND	ND
		Pyrene	97.05 ± 0.27	525.48 ± 180	64.63 ± 33.22
Proteomonas sp.	27.09 ± 1.2	Phenanthrene	1.19 ± 0.18	178.4 ± 30	ND
		Pyrene	39.58 ± 5.7	ND	325.32 ± 124.67

Table 1: Differences in lipid content (mean ± SE, n = 3), the maximum percentage of cells (mean ± SE) showing positive PAH sorption (48-h), PAH lethal concentrations (LC_{10} ± SE), and EC_{10} values (mean ± SE) for F_v/F_m between the three studied phytoplankton species. ND: not determined.

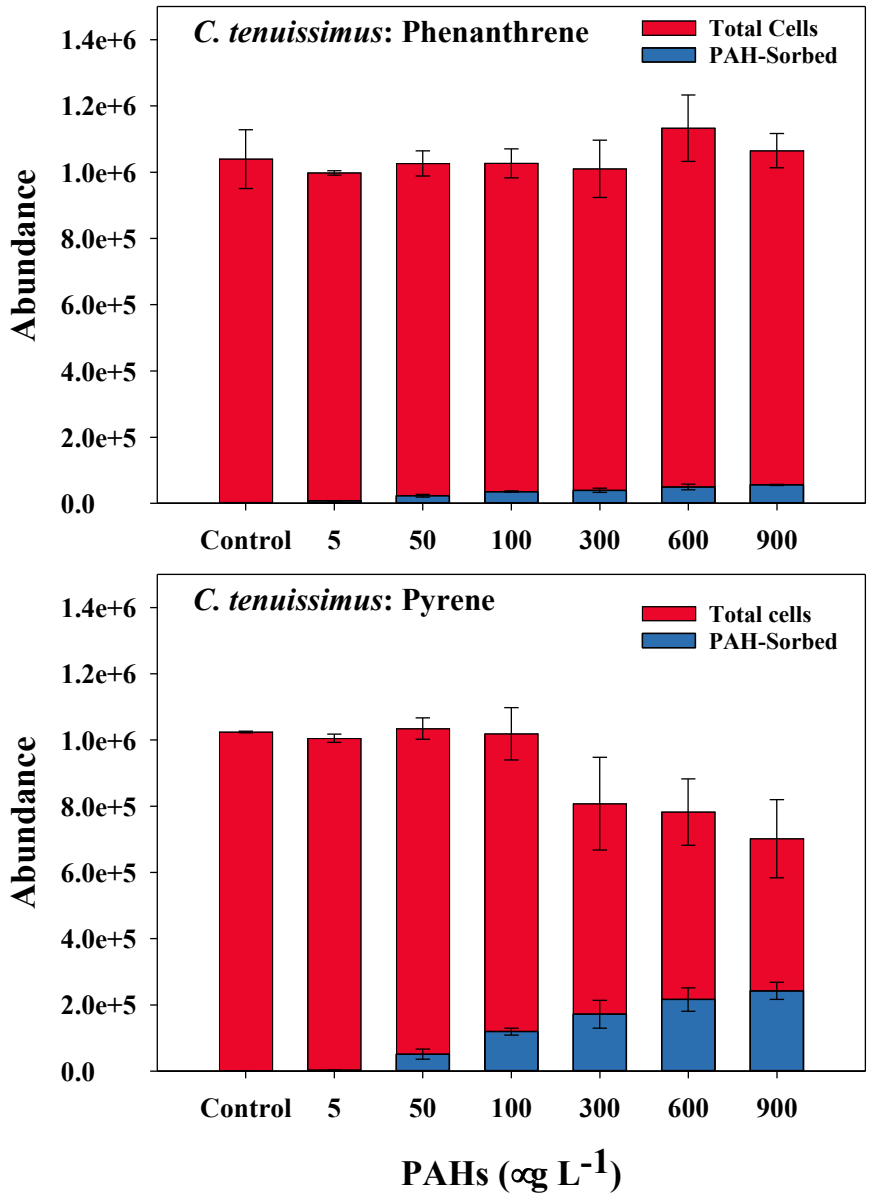

254

255 **Fig. 1**. Proportion of *Chaetoceros tenuissimus* cells showing phenanthrene and pyrene

256 sorption after a 48-h dosage schedule, measured by 375 nm UV excitation flow cytometry.

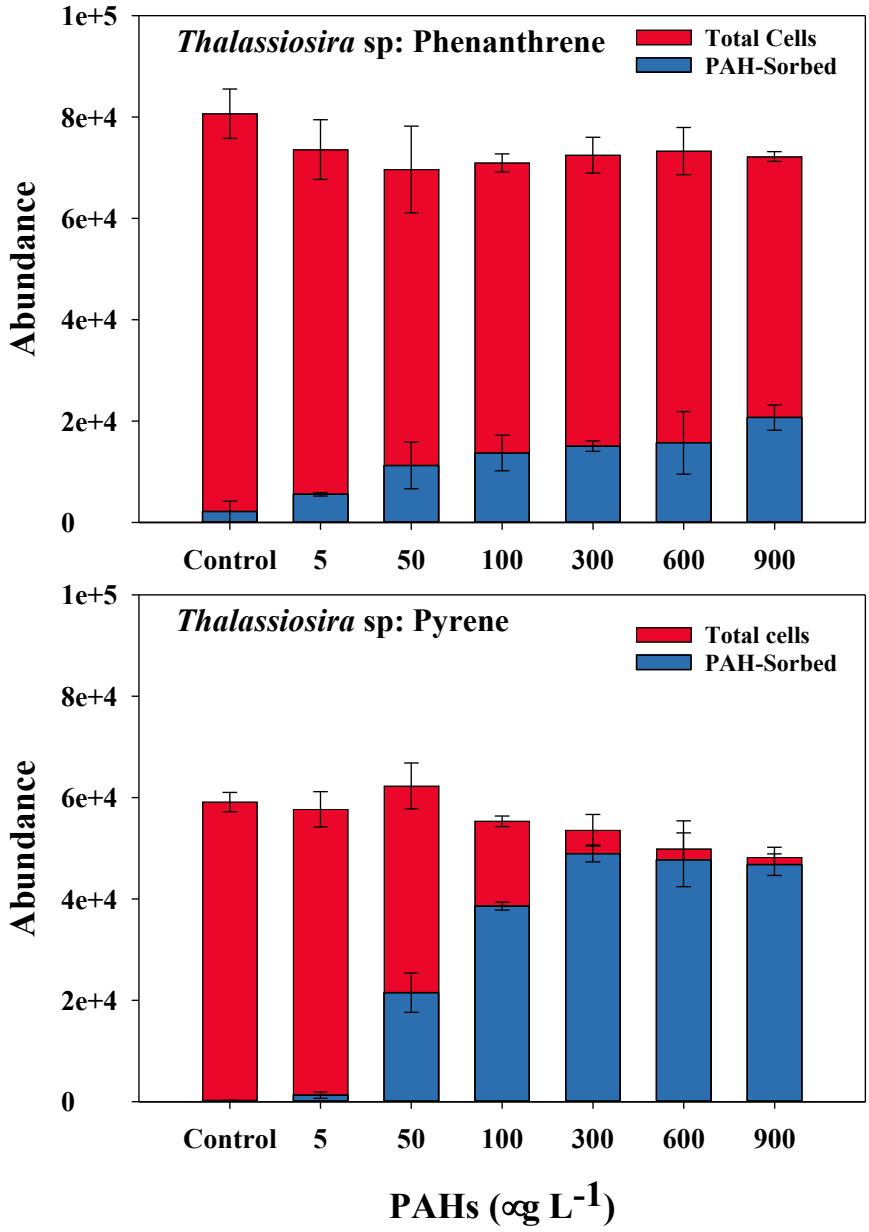

257

258 **Fig. 2**. Proportion of *Thalassiosira* sp. cells showing phenanthrene and pyrene sorption after

259 a 48-h dosage schedule, measured by 375 nm UV excitation flow cytometry.

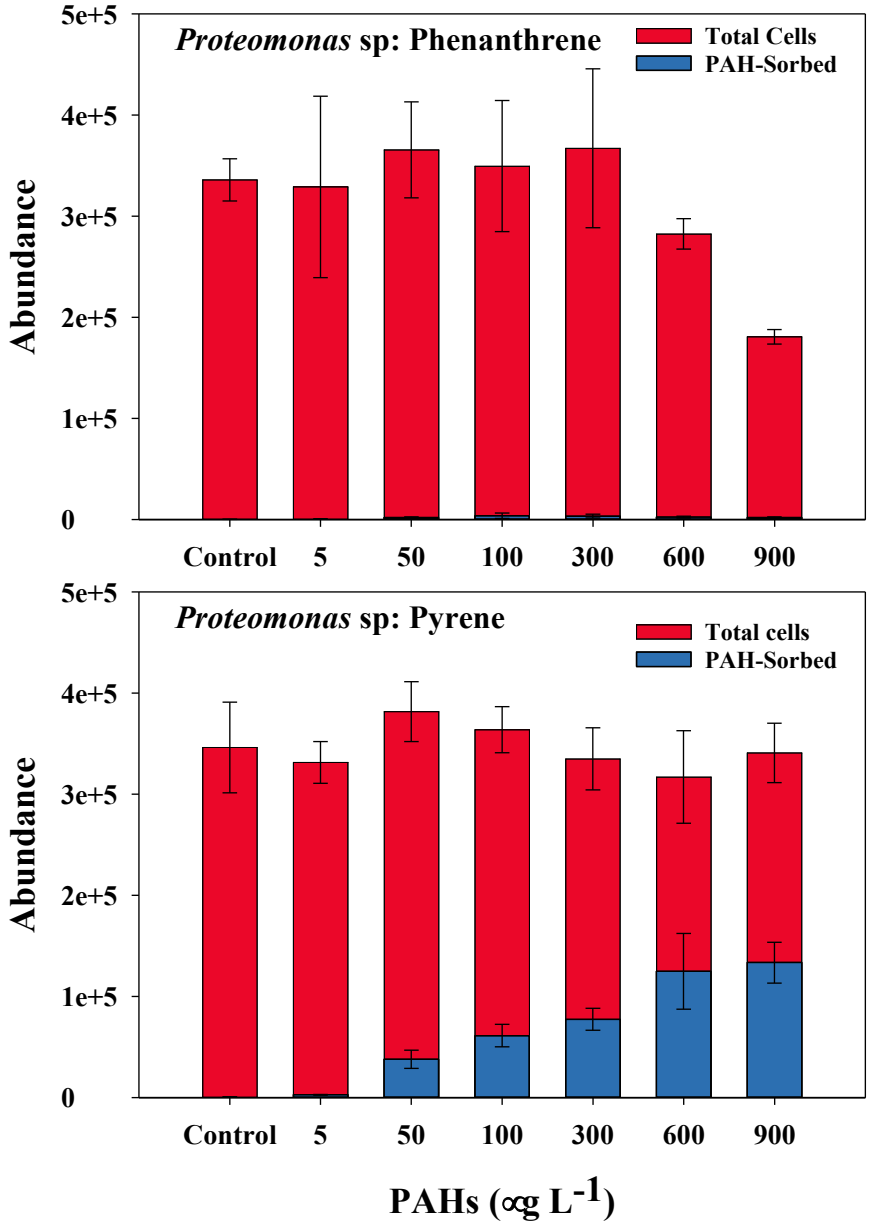

Fig. 3. Proportion of *Proteomonas* sp. cells showing phenanthrene and pyrene sorption after a 48-h dosage schedule, measured by 375 nm UV excitation flow cytometry.

In *Thalassiosira* sp., where the maximum PAH sorption was detected, we explored the temporal changes in PAH sorption over 6−96 h periods (**Fig. 4**). We found a dose-dependent rapid sorption of pyrene, with 58% and 84% cells showing positive PAH fluorescence within 6 hours of exposure to 50 µg L^{-1} and 100 µg L^{-1}, respectively, while over 95% of cells were

pyrene-sorbed at concentrations above 300 µg L^{-1}. Moreover, for all tested doses, the highest percentage of pyrene sorption was observed within the first 24 h of exposure, beyond which there was a decline, which was more significant at sublethal doses of 50 µg L^{-1} and 100 µg L^{-1} ($p < 0.001$). Daily growth rates showed a stimulatory effect of lower doses of pyrene (Supplementary materials S1), and the cultures exhibited adequate growth rates up to 100 µg L^{-1} throughout the exposure period.

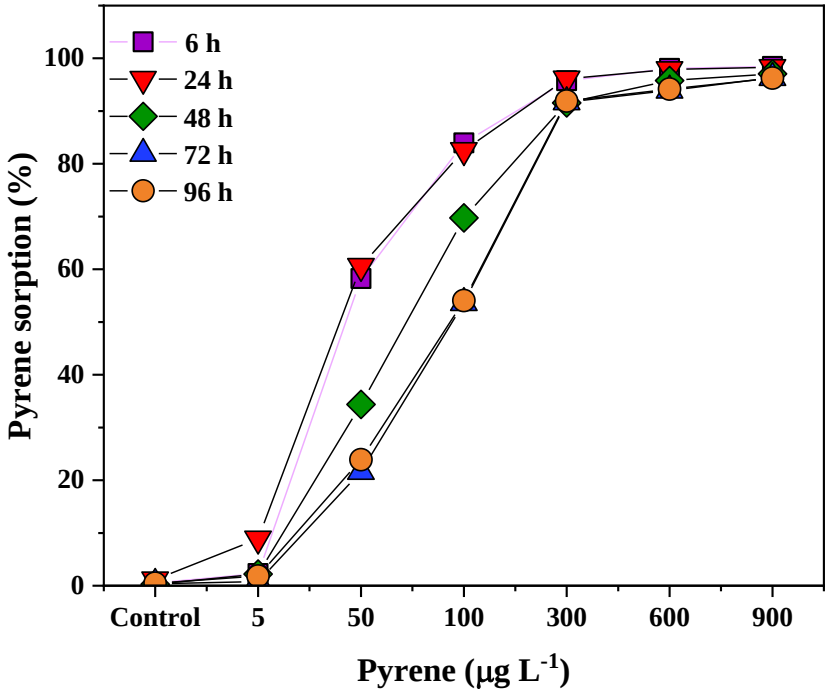

Fig. 4. Temporal changes in pyrene sorption by *Thalassiosira* sp. cells over a 6−96 h period measured by 375 nm UV excitation flow cytometry.

3.2 Epifluorescence microscopy and M-PAM analysis

Epifluorescence microscopy revealed the cellular sorption of PAHs from the medium as bright blue fluorescent blots (**Fig. 5**). The lower magnitude of phenanthrene sorption, as revealed by flow cytometry analyses, was verified by the microscopy counts. Out of several

hundred cells of each species counted, none of them showed the anticipated blue fluorescence emission under UV irradiance. However, at dosages above 100 μg L^{-1}, pyrene exposed cells showed significant records of blue fluorescent cells, up to 3%, 15%, and 90% for *C. tenuissimus*, *Proteomonas* sp., and *Thalassiosira* sp., respectively (**Fig. 6**). The proportion of blue fluorescent cells at higher doses of pyrene was similar between *C. tenuissimus* and *Proteomonas* sp. At concentrations above 300 μg L^{-1}, all *Thalassiosira* cells in the suspension were blue fluorescing, indicating the absolute and uniform sorption of the toxicant onto the cells. Moreover, the percentage of microscopic counts of the pyrene sorption were well correlated with that of the flow cytometric counts in all of the phytoplankton species analyzed (*C. tenuissimus*: $r^2 = 0.94$, $p = 0.0003$; *Thalassiosira* sp: $r^2 = 0.86$, $p = 0.0028$; *Proteomonas* sp: $r^2 = 0.84$, $p = 0.0037$).

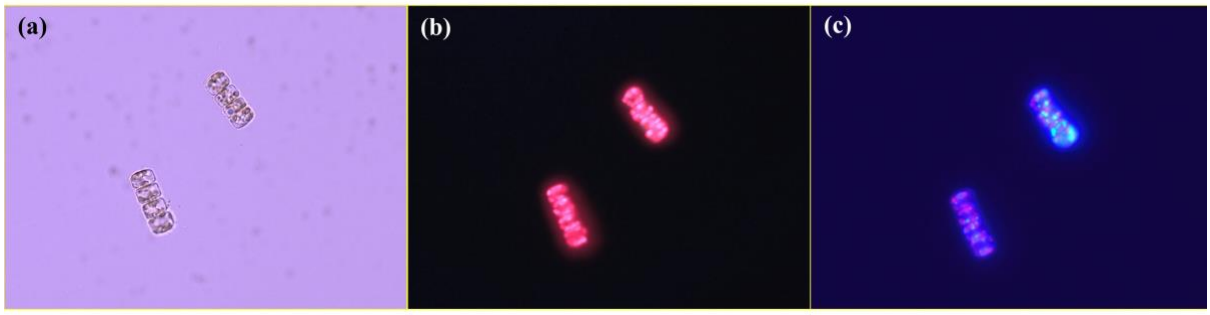

Fig. 5. Light microscope (a) and epifluorescence microscope (b, c) images of *Thalassiosira* sp. showing chlorophyll red fluorescence (b) and bright blue fluorescent blotches of sorbed pyrene (c, from 900 μg L^{-1} treatment).

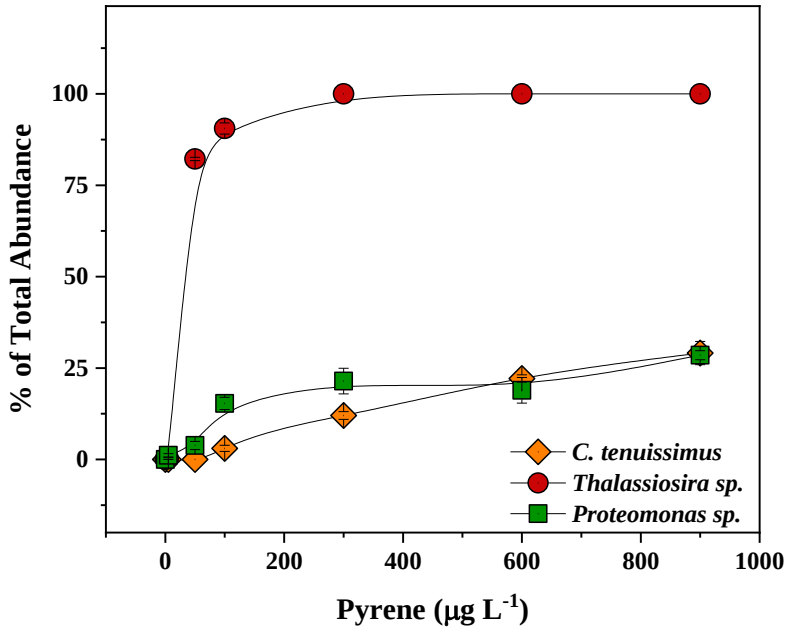

297

298 **Fig. 6**. Percentage of pyrene sorption in three phytoplankton taxa after a 48-h dosing
299 schedule, estimated by 365 nm UV excitation microscopy counting method.

300 Cell-by-cell comparison of F_v/F_m between PAH-sorbed and normal cells revealed the
301 physiological effect of PAH sorption in the studied phytoplankton. Phenanthrene did not
302 show any effect on the photosynthetic performance of the treated cells, except in
303 *Proteomonas* sp. at 900 µg L^{-1}, where we observed a reduction of 14% in the control values.
304 However, for pyrene, all the taxa exhibited significant declines in F_v/F_m (**Fig. 7**),
305 corresponding to the cellular sorption. We observed over 50% reductions in F_v/F_m at dosages
306 above 600 µg L^{-1} for *C. tenuissimus* (ANOVA, $df = 6$, $F = 40.81$, $p < 0.0001$), 300 µg L^{-1} for
307 *Thalassiosira* (ANOVA, $df = 6$, $F = 25.72$, $p < 0.0001$), and 300 µg L^{-1} for *Proteomonas*
308 (ANOVA, $df = 6$, $F = 14$, $p < 0.0001$). We also observed a significant difference among the
309 two tested classes of phytoplankton, with the cryptophyte being more sensitive to higher
310 doses of pyrene, causing up to an 82% reduction in F_v/F_m. However, the EC_{10} values were
311 lower for the diatoms (**Table 1**). The M-PAM measurements revealed the exact physiological

consequence of PAH sorption on phytoplankton photosynthesis, as shown here, for example, by the high correlation between the reduction in F_v/F_m and pyrene sorption in *C. tenuissimus* ($r^2 = 0.98$, $p < 0.0001$) and *Proteomonas* ($r^2 = 0.85$, $p < 0.0001$).

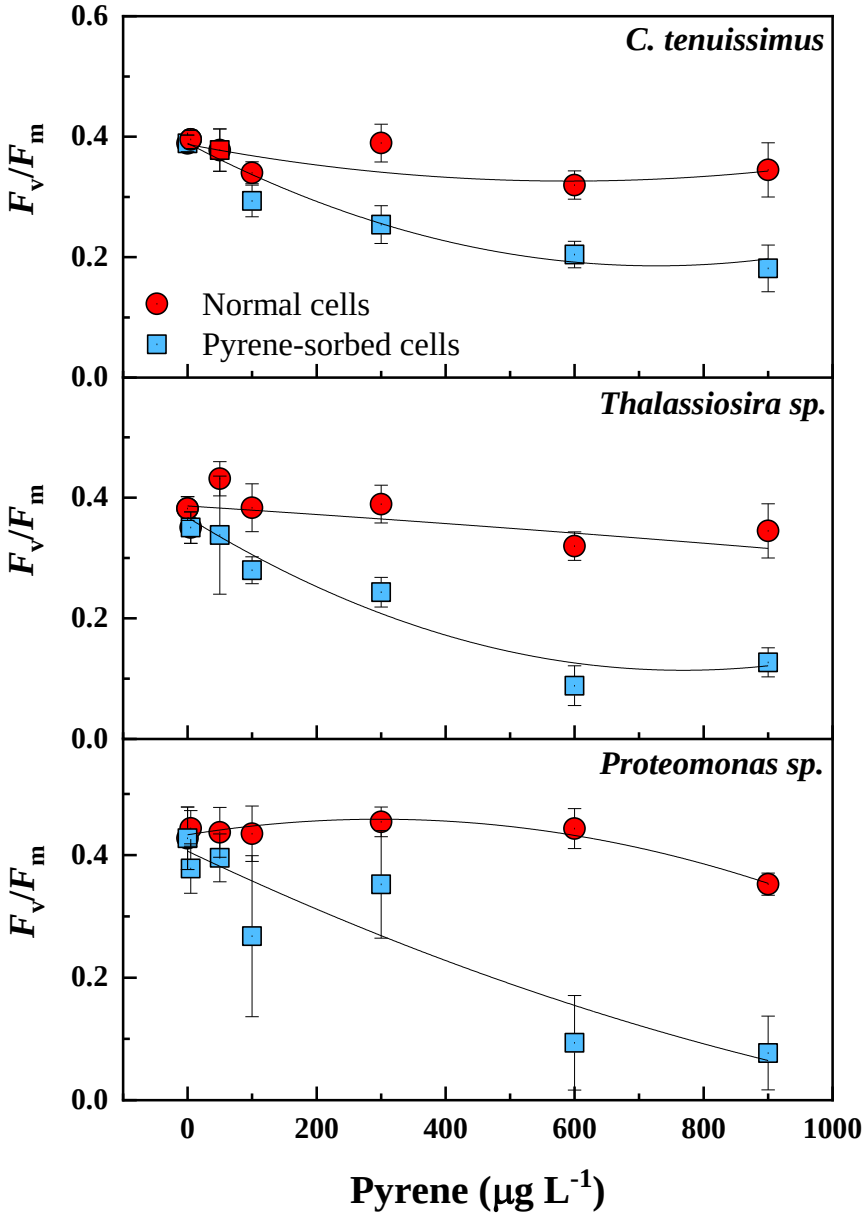

Fig. 7. Selective pressure of pyrene on F_v/F_m of sorbed and normal cells of three phytoplankton taxa measured by single cell-level microscopy PAM method.

3.3 Total lipid contents

Gravimetric estimation of total lipids revealed significantly different levels in the three phytoplankton species studied (**Table 1**). *Thalassiosira* sp. showed the highest amount of intracellular lipids (33.87% DW) and the lowest amounts in *C. tenuissimus* (7.22% DW). The species with the highest lipid levels showed the maximum PAH surface sorption, more significantly in the case of pyrene.

Spearman coefficient analysis revealed statistically significant correlations between lipid level and cellular sorption of phenanthrene (ρ = +0.474; p = 0.001), and pyrene (ρ = +0.719; $p < 0.0001$) (**Fig. 8**). A stronger correlation was observed for pyrene, which showed higher sorption by all the three tested species.

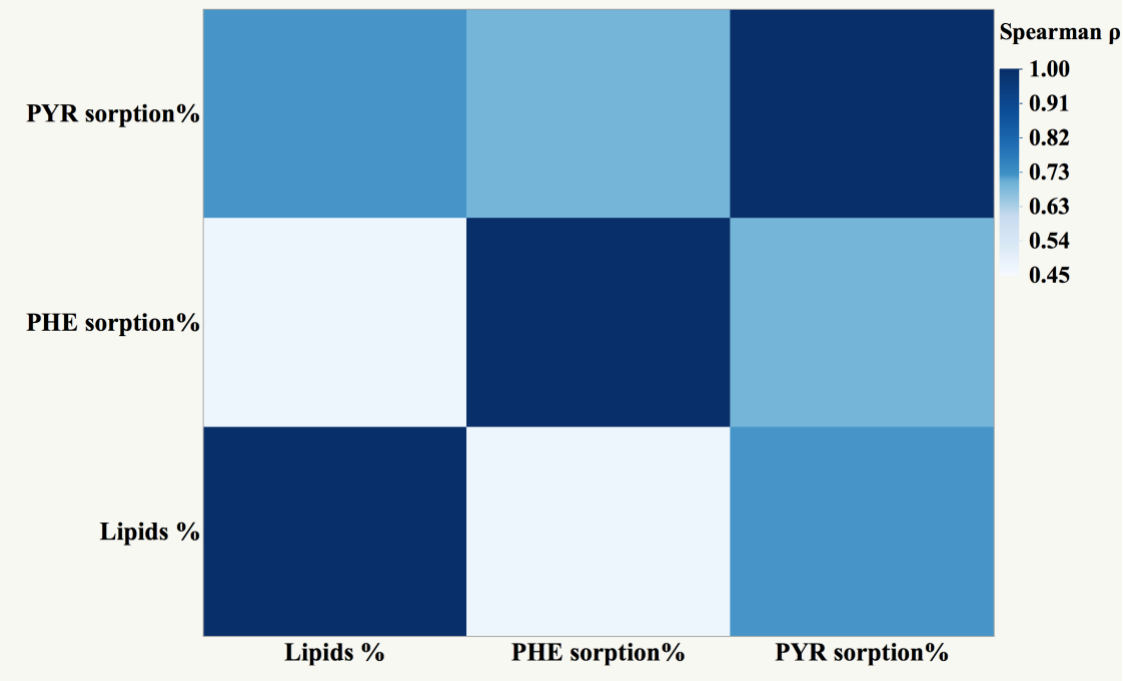

Fig. 8. Spearman's correlation heatmap showing relationship between lipid content and sorption levels of phenanthrene (PHE) and pyrene (PYR) in three test phytoplankton species.

4. Discussion

In phytoplankton suspensions exposed to two PAHs, we identified and quantified the discrete cells that accumulated PAHs from the dissolved phase in the seawater medium, based on the characteristic blue fluorescence emission of the PAHs. Significant progress in the application of flow cytometry in aquatic ecotoxicological research has led to the development of feasible test methods that have fewer sample requirements and simple preparation methods (Cerezo et al., 2017; Kottuparambil & Agusti, 2018; Prado et al., 2015). Generally, these methods track intrinsic features of individual cells within a population, such as autofluorescence or dimension (Hyka et al., 2013). With the introduction of fluorescent physiological dyes, flow cytometry has been rapidly developed as a state-of-the-art technique in phytoplankton research (Croxton et al., 2015; Fachet et al., 2016). Single cell-level phytoplankton toxicity assessment based on confocal microscopy and digital imaging has also proven to be superior to conventional tests because it permits the use of environmentally relevant algal densities and toxicant concentrations (Nancharaiah et al., 2007). Recently, a hybrid technology of imaging flow cytometry, which combines the visualization potential of fluorescence microscopy with the statistical power of flow cytometry, has emerged as a promising analytical tool (Dashkova et al., 2017). However, despite these technological advances, the use of flow cytometry has been limited in ecotoxicological studies of fluorescent xenobiotics in marine environments.

Here, we introduce a novel approach to detect the extent of PAH binding onto individual phytoplankton cells in a suspension and precisely evaluate the inhibitory effects of PAH binding on the photosynthetic capacity of individual cells. We employed the flow cytometry method of detecting PAHs-sorbed cells (Cerezo et al., 2017), which was relatively rapid and straightforward, and showed a good correlation with the manual counts obtained by an epifluorescence microscope. We detected up to 29% and 97% of cells in the *Thalassiosira* sp.

suspension with significant sorption of phenanthrene and pyrene, respectively. Pyrene showed a higher binding affinity than phenanthrene, which may be due to differences in the toxicity potential, bioavailability, and their mode of interaction at the cell membranes. Moreover, pyrene has four aromatic benzene rings. Consequently, it has a higher fluorescence emission than the three-ringed phenanthrene (Zhang et al., 2015), which allows for easier detection by the flow cytometer. However, in general, we found that PAH accumulation resulted in a negligible corresponding significant decline in growth, indicating either active detoxifying mechanisms or alternate physiological targets of the toxicants. Furthermore, in *Thalassiosira* sp., daily growth rates over a 96-h period clearly showed that a high cell growth rate helped to reduce the pyrene sorption over time due to dilution of the toxicant and a simultaneous increase in the biomass. In general, diatoms exhibit relatively high tolerance to low doses of PAHs, and this tolerance decreases with higher concentrations (González et al., 2009). At similar doses of pyrene to our experiments, a gene expression study in *Thalassiosira pseudonana* reported significant effects on fatty acid metabolism, silica shell formation, and photosynthesis, without eliciting growth inhibition (Bopp & Lettieri, 2007). Therefore, our data suggest that the physiological and molecular targets of pollutants in aquatic organisms should be taken into consideration when developing environmental risk assessment guidelines.

We attribute the variation in PAH-sorption profiles among the three tested taxa reported here to differences in the biochemical characteristics of the organisms. PAHs are lipophilic, and the final destination of these PAH compounds in algal cells is lipid vesicles (Augusto et al., 2015; Subashchandrabose et al., 2014). The porous cell wall surrounding the diatom cells allows PAHs to come into contact with the plasma membrane, eventually redistributing among the different internal lipid pools because of their hydrophobicity (Carvalho et al., 2011). We observed the sorbed pyrene as clear blue fluorescent globules inside *Thalassiosira*

cells (**Fig. 5**). Moreover, there was a strong and significant positive correlation ($p < 0.0001$) between lipid content and pyrene sorption (**Fig. 8**). Hence, the high pyrene accumulation in *Thalassiosira* sp. evidently corresponds to its high intercellular lipid levels compared to the other two taxa (385% and 26% more than those in *C. tenuissimus* and *Proteomonas* sp., respectively). The high lipid content can also be a protective strategy for the organism where lipophilic xenobiotics are sequestered, thus reducing their bioavailability and toxicity (Yang et al., 2002).

The flow cytometry measurements conducted over the incubation period (6−96 h) in *Thalassiosira* sp. revealed the rapid sorption of pyrene at higher concentrations tested (> 300 μg L^{-1}), with over 90% of pyrene sorbed by cells within 6 h of exposure. Pyrene sorption reached a maximum within the first 24 h of exposure; however, cellular growth at the lower tested concentrations (5−100 μg L^{-1}) resulted in a gradual decline in the amount of the sorbed pyrene at the cell surface due to the dilution effect with increasing abundance. Corresponding to the distinct positive correlation between lipid level and PAH sorption (**Fig. 8**), the rapid accumulation of hydrophobic pyrene is likely facilitated by the high lipid content of *Thalassiosira* sp. (**Table 1**). The lipid globules act as localized sites for PAH sorption, forming toxicant-concentrated bright blots as shown in the fluorescence images (**Fig. 5**). These globules produce strong PAH-fluorescence signals during the flow cytometry detection, which in turn produces the high PAH sorption shown by *Thalassiosira* sp. Our flow cytometry method allows for more rapid, selective, and accurate detection of PAH accumulation relative to other conventional methods that involve chemical analyses of the toxicants.

Microscopy PAM provides cell-specific, robust, and real-time measurement of phytoplankton physiology. This method has been used to predict phytoplankton succession and blooming (Higo et al., 2017), photophysiological characterization (Villareal & Morton, 2002), and

herbicide toxicity assessment (Schmitt-Jansen & Altenburger, 2007). Chlorophyll fluorescence-based estimation of microalgal photosynthetic variables in toxicity assays usually relies on whole suspension measurements that obscure differences among individual cells. The sub-lethal effects of PAHs on marine phytoplankton photosynthesis are well documented, both at population and community levels (Pérez et al., 2010). However, the mechanism of PAH toxicity in phytoplankton photosynthesis remains ambiguous because different species show contrasting photosynthetic responses (Ben Othman et al., 2018; Othman et al., 2012). By measuring at the single-cell level, our data revealed a significant decrease in F_v/F_m for phytoplankton exposed to pyrene, with different thresholds, suggesting a general degradation of PSII efficiency (**Fig. 7**). F_v/F_m denotes the potential quantum yield of PSII when all PSII reaction centers are open, and the excitation energy is primarily diverted to the photosynthetic reactions (Bilger et al., 1995). The response of F_v/F_m depends on the toxicity mechanism of the specific pollutant, and earlier studies have indicated that PAHs primarily impact the PSII reaction centers in phytoplankton (Shao et al., 2010). By distinguishing photosynthetically active and inactive cells, our data clearly demonstrate the selective adverse effects of PAHs on PAH-sorbed cells. In contrast, the unaffected cells can continue to perform photosynthesis optimally. This observation is particularly significant as it reveals the actual response of individual organisms to pollutants, which generally are biased in population-level toxicity assessments by the intense fluorescence signals that overlook unaffected healthy cells. Obviously, the PAH-sorbed cells have reduced physiological capacity, and most likely affect the population growth pattern at higher doses of PAHs upon longer exposures. The reduced photosynthetic performance of a subset of the population can also result in a significant parallel decrease in primary production (González et al., 2009). Moreover, the PAH-sorbed cells continue to act as a carrier of the toxicants for certain periods, thus providing closed sites for bacterial degradation (Gutierrez et al., 2012) or

434 expediting the trophic transfer of these toxicants to grazers through the food chain
435 (Berrojalbiz et al., 2009).

436 Duration of exposure to toxicants determines the severity and extent of the cytotoxic response
437 in phytoplankton model tests. From our observations, we recommend a 24 h exposure time
438 for short-term flow cytometry screening of fluorescent toxicants in phytoplankton. This
439 duration optimally minimizes the complications due to volatilization and degradation of
440 toxicants, and the loss due to binding to the test vessel walls. In the case of pyrene, with a
441 relatively high log K_{ow} value of 5.20 (Bayona et al., 1991) than that of phenanthrene (4.6), we
442 observed maximum sorption levels within 24 h. Beyond this time point, the exposure
443 conditions change considerably which can alter the flow cytometry output significantly,
444 unless the exposure concentrations are constantly adjusted.

445 Our observations emphasize that, apart from lethal toxicity targets, PAHs can interact with
446 other vital cellular processes, thus prompting significant sub-lethal effects in phytoplankton.
447 Although we tested two PAHs at concentrations much higher than those found in the open
448 ocean, our experimental approach delivered ecologically relevant information on the fate of
449 toxic fluorescing chemicals in marine systems. The physiological insights of microscopy
450 PAM combined with the powerful optical detection system of flow cytometry allowed us to
451 estimate the impact of tested PAHs in phytoplankton accurately. To the best of our
452 knowledge, this is the first study to report a selective investigation on the impacts of PAHs on
453 a more relevant subset of affected (PAH-sorbed) phytoplankton cells in a suspension. Our
454 flow cytometry method is potentially useful to estimate the ecotoxicity of fluorescent
455 aromatic compounds in coastal areas prone to hydrocarbon contamination. The method
456 outlined here has definite advantages over traditional population-level methods in terms of
457 ecological relevance of the results because cell-by-cell measurements yield a more precise
458 depiction of individual cell responses to chemical stress. Moreover, the combination of flow

cytometry and microscopy-PAM tools offers a fast, robust, and sensitive hybrid technology to detect the harmful effects of fossil fuel-derived toxicants in a vital ecosystem of the marine environment. Further studies are potentially promising to demonstrate the applicability of this technique to other test models such as bacteria and cell lines.

Acknowledgements

This study was funded by the King Abdullah University of Science and Technology (KAUST) through baseline funding BAS/1/1072–01–01 to SA. We thank Juan D. Martinez Ayala for his assistance in isolation of the phytoplankton species, Dr. Francisco L. Aparicio Bernat for maintenance of the algal cultures, Gala Gonzalez for carrying out the lipid analysis, and Malak Abdullah for help in flow cytometry analysis.

CRediT authorship contribution statement:

Sreejith Kottuparambil: Methodology, Investigation, Validation, Formal analysis, Visualization, Writing - original draft, Writing - review & editing. **Susana Agusti**: Conceptualization, Resources, Funding acquisition, Supervision, Project management, Writing - review & editing.

Competing interests

The authors declare that they have no known competing financial interests or personal relationships that could have appeared to influence the work reported in this paper.

Human/animal rights statements and informed consent

No conflicts, informed consent, human, or animal rights applicable.

References

Al-Mur, B.A. 2019. Assessing the ecological risks from hydrocarbons in the marine coastal sediments of Jeddah, Red Sea. *Environmental monitoring and assessment*, **191**(3), 180.

Alves, W.S., Manoel, E.A., Santos, N.S., Nunes, R.O., Domiciano, G.C., Soares, M.R. 2017. Detection of polycyclic aromatic hydrocarbons (PAHs) in Medicago sativa L. by fluorescence microscopy. *Micron*, **95**, 23-30.

Anglès, S., Jordi, A., Campbell, L. 2015. Responses of the coastal phytoplankton community to tropical cyclones revealed by high-frequency imaging flow cytometry. *Limnology and Oceanography*, **60**(5), 1562-1576.

Augusto, S., Sierra, J., Nadal, M., Schuhmacher, M. 2015. Tracking polycyclic aromatic hydrocarbons in lichens: It's all about the algae. *Environmental Pollution*, **207**, 441-445.

Bayona, J., Fernandez, P., Porte, C., Tolosa, I., Valls, M., Albaiges, J.J.C. 1991. Partitioning of urban wastewater organic microcontaminants among coastal compartments. **23**(3), 313-326.

Ben Othman, H., Lanouguère, É., Got, P., Sakka Hlaili, A., Leboulanger, C. 2018. Structural and functional responses of coastal marine phytoplankton communities to PAH mixtures. *Chemosphere*, **209**, 908-919.

Berrojalbiz, N., Lacorte, S., Calbet, A., Saiz, E., Barata, C., Dachs, J. 2009. Accumulation and Cycling of Polycyclic Aromatic Hydrocarbons in Zooplankton. *Environmental Science & Technology*, **43**(7), 2295-2301.

506 Bilger, W., Schreiber, U., Bock, M. 1995. Determination of the quantum efficiency of
507 photosystem II and of non-photochemical quenching of chlorophyll fluorescence in
508 the field. *Oecologia*, **102**(4), 425-432.

509 Bopp, S.K., Lettieri, T. 2007. Gene regulation in the marine diatom Thalassiosira pseudonana
510 upon exposure to polycyclic aromatic hydrocarbons (PAHs). *Gene*, **396**(2), 293-302.

511 Carvalho, R.N., Burchardt, A.D., Sena, F., Mariani, G., Mueller, A., Bopp, S.K., Umlauf, G.,
512 Lettieri, T. 2011. Gene biomarkers in diatom Thalassiosira pseudonana exposed to
513 polycyclic aromatic hydrocarbons from contaminated marine surface sediments.
514 *Aquatic Toxicology*, **101**(1), 244-253.

515 Cerezo, M.I., Agustí, S. 2015. PAHs reduce DNA synthesis and delay cell division in the
516 widespread primary producer Prochlorococcus. *Environmental Pollution*, **196**, 147-
517 155.

518 Cerezo, M.I., Linden, M., Agustí, S. 2017. Flow cytometry detection of planktonic cells with
519 polycyclic aromatic hydrocarbons sorbed to cell surfaces. *Marine Pollution Bulletin*,
520 **118**(1), 64-70.

521 Croxton, A.N., Wikfors, G.H., Schulterbrandt-Gragg, R.D. 2015. The use of flow cytometric
522 applications to measure the effects of PAHs on growth, membrane integrity, and
523 relative lipid content of the benthic diatom, Nitzschia brevirostris. *Marine Pollution*
524 *Bulletin*, **91**(1), 160-165.

525 Cyr, F., Tedetti, M., Besson, F., Bhairy, N., Goutx, M. 2019. A Glider-Compatible Optical
526 Sensor for the Detection of Polycyclic Aromatic Hydrocarbons in the Marine
527 Environment. *Frontiers in Marine Science*, **6**(110).

528 Dashkova, V., Malashenkov, D., Poulton, N., Vorobjev, I., Barteneva, N.S. 2017. Imaging
529 flow cytometry for phytoplankton analysis. *Methods*, **112**, 188-200.

530 Echeveste, P., Galbán-Malagón, C., Dachs, J., Berrojalbiz, N., Agustí, S. 2016. Toxicity of
531 natural mixtures of organic pollutants in temperate and polar marine phytoplankton.
532 *Science of The Total Environment*, **571**, 34-41.

533 Fachet, M., Hermsdorf, D., Rihko-Struckmann, L., Sundmacher, K. 2016. Flow cytometry
534 enables dynamic tracking of algal stress response: A case study using carotenogenesis
535 in Dunaliella salina. *Algal Research*, **13**, 227-234.

536 Ferrante, M., Zanghì, G., Cristaldi, A., Copat, C., Grasso, A., Fiore, M., Signorelli, S.S.,
537 Zuccarello, P., Oliveri Conti, G. 2018. PAHs in seafood from the Mediterranean Sea:
538 An exposure risk assessment. *Food and Chemical Toxicology*, **115**, 385-390.

539 Folch, J., Lees, M., Sloane Stanley, G. 1957. A simple method for the isolation and
540 purification of total lipides from animal tissues. *J biol Chem*, **226**(1), 497-509.

541 Franklin, N.M., Stauber, J.L., Lim, R.P. 2001. Development of flow cytometry-based algal
542 bioassays for assessing toxicity of copper in natural waters. *Environmental toxicology*
543 *and chemistry*, **20**(1), 160-170.

544 Franklin, N.M., Stauber, J.L., Lim, R.P. 2004. Development of multispecies algal bioassays
545 using flow cytometry. *Environmental Toxicology and Chemistry*, **23**(6), 1452-1462.

546 Froehner, S., Maceno, M., Machado, K.S. 2011. Predicting bioaccumulation of PAHs in the
547 trophic chain in the estuary region of Paranagua, Brazil. *Environmental Monitoring*
548 *and Assessment*, **174**(1), 135-145.

549 Gérikas Ribeiro, C., Lopes dos Santos, A., Marie, D., Pereira Brandini, F., Vaulot, D. 2018.
550 Small eukaryotic phytoplankton communities in tropical waters off Brazil are
551 dominated by symbioses between Haptophyta and nitrogen-fixing cyanobacteria. *The*
552 *ISME Journal*, **12**(5), 1360-1374.

553 Goh, C.-H., Schreiber, U., Hedrich, R. 1999. New approach of monitoring changes in
554 chlorophyll a fluorescence of single guard cells and protoplasts in response to
555 physiological stimuli. *Plant, Cell & Environment*, **22**(9), 1057-1070.

556 González, J., Figueiras, F.G., Aranguren-Gassis, M., Crespo, B.G., Fernández, E., Morán,
557 X.A.G., Nieto-Cid, M. 2009. Effect of a simulated oil spill on natural assemblages of
558 marine phytoplankton enclosed in microcosms. *Estuarine, Coastal and Shelf Science*,
559 **83**(3), 265-276.

560 González-Gaya, B., Fernández-Pinos, M.-C., Morales, L., Méjanelle, L., Abad, E., Piña, B.,
561 Duarte, C.M., Jiménez, B., Dachs, J. 2016. High atmosphere–ocean exchange of
562 semivolatile aromatic hydrocarbons. *Nature Geoscience*, **9**(6), 438.

563 Gutierrez, T., Nichols, P.D., Whitman, W.B., Aitken, M.D. 2012. Porticoccus
564 hydrocarbonoclasticus sp. nov., an aromatic hydrocarbon-degrading bacterium
565 identified in laboratory cultures of marine phytoplankton. *Appl. Environ. Microbiol.*,
566 **78**(3), 628-637.

567 Hayakawa, K. 2018. Polycyclic Aromatic Hydrocarbons in the Southeastern Japan Sea. in:
568 *Polycyclic Aromatic Hydrocarbons: Environmental Behavior and Toxicity in East*
569 *Asia*, (Ed.) K. Hayakawa, Springer Singapore. Singapore, pp. 203-211.

570 Higo, S., Maung Saw Htoo, T., Yamatogi, T., Ishida, N., Hirae, S., Koike, K. 2017.
571 Application of a pulse-amplitude-modulation (PAM) fluorometer reveals its

usefulness and robustness in the prediction of Karenia mikimotoi blooms: A case study in Sasebo Bay, Nagasaki, Japan. *Harmful Algae*, **61**, 63-70.

Hyka, P., Lickova, S., Přibyl, P., Melzoch, K., Kovar, K. 2013. Flow cytometry for the development of biotechnological processes with microalgae. *Biotechnology Advances*, **31**(1), 2-16.

Ke, C.-L., Gu, Y.-G., Liu, Q., Li, L.-D., Huang, H.-H., Cai, N., Sun, Z.-W. 2017. Polycyclic aromatic hydrocarbons (PAHs) in wild marine organisms from South China Sea: Occurrence, sources, and human health implications. *Marine Pollution Bulletin*, **117**(1), 507-511.

Kottuparambil, S., Agusti, S. 2018. PAHs sensitivity of picophytoplankton populations in the Red Sea. *Environmental Pollution*, **239**, 607-616.

Liu, K., Dickhut, R.M. 1997. Surface Microlayer Enrichment of Polycyclic Aromatic Hydrocarbons in Southern Chesapeake Bay. *Environmental Science & Technology*, **31**(10), 2777-2781.

Nancharaiah, Y.V., Rajadurai, M., Venugopalan, V.P. 2007. Single Cell Level Microalgal Ecotoxicity Assessment by Confocal Microscopy and Digital Image Analysis. *Environmental Science & Technology*, **41**(7), 2617-2621.

Othman, H.B., Leboulanger, C., Le Floc'h, E., Hadj Mabrouk, H., Sakka Hlaili, A. 2012. Toxicity of benz(a)anthracene and fluoranthene to marine phytoplankton in culture: Does cell size really matter? *Journal of Hazardous Materials*, **243**, 204-211.

Pena, E.A., Ridley, L.M., Murphy, W.R., Sowa, J.R., Bentivegna, C.S. 2015. Detection of polycyclic aromatic hydrocarbons (PAHs) in raw menhaden fish oil using

fluorescence spectroscopy: Method development. *Environmental Toxicology and Chemistry*, **34**(9), 1946-1958.

Penko, L., Bajt, O. 2019. Aliphatic and polycyclic aromatic hydrocarbons in surface seawater of the GULF of Trieste (northern ADRIATIC). *Marine Pollution Bulletin*, **142**, 103-111.

Pérez, P., Fernández, E., Beiras, R. 2010. Use of Fast Repetition Rate Fluorometry on Detection and Assessment of PAH Toxicity on Microalgae. *Water, Air, & Soil Pollution*, **209**(1), 345-356.

Poster, D.L., Schantz, M.M., Sander, L.C., Wise, S.A.J.A., Chemistry, B. 2006. Analysis of polycyclic aromatic hydrocarbons (PAHs) in environmental samples: a critical review of gas chromatographic (GC) methods. **386**(4), 859-881.

Prado, R., García, R., Rioboo, C., Herrero, C., Cid, Á. 2015. Suitability of cytotoxicity endpoints and test microalgal species to disclose the toxic effect of common aquatic pollutants. *Ecotoxicology and Environmental Safety*, **114**, 117-125.

Qari, H.A., Hassan, I.A. 2017. Bioaccumulation of PAHs in Padina boryana Alga Collected from a Contaminated Site on the Red Sea, Saudi Arabia. *Polish Journal of Environmental Studies*, **26**(1).

Ramalhosa, M.J., Paíga, P., Morais, S., Ramos, S., Delerue-Matos, C., Oliveira, M.B.P.P. 2012. Polycyclic aromatic hydrocarbon levels in three pelagic fish species from Atlantic Ocean: Inter-specific and inter-season comparisons and assessment of potential public health risks. *Food and Chemical Toxicology*, **50**(2), 162-167.

615 Rodriguez, J.S., Sanz, C.P. 2000. Fluorescence techniques for the determination of polycyclic
616 aromatic hydrocarbons in marine environment: an overview. *Analusis*, **28**(8), 710-
617 717.

618 Rutten, T.P.A., Sandee, B., Hofman, A.R.T. 2005. Phytoplankton monitoring by high
619 performance flow cytometry: A successful approach? *Cytometry Part A*, **64A**(1), 16-
620 26.

621 Sarrazin, L., Diana, C., Wafo, E., Pichard-Lagadec, V., Schembri, T., Monod, J.L. 2006.
622 Determination of Polycyclic Aromatic Hydrocarbons (PAHs) in Marine, Brackish,
623 and River Sediments by HPLC, Following Ultrasonic Extraction. *Journal of Liquid*
624 *Chromatography & Related Technologies*, **29**(1), 69-85.

625 Schmitt-Jansen, M., Altenburger, R. 2007. The use of pulse-amplitude modulated (PAM)
626 fluorescence-based methods to evaluate effects of herbicides in microalgal systems of
627 different complexity. *Toxicological & Environmental Chemistry*, **89**(4), 665-681.

628 Schreiber, U., Bilger, W., Neubauer, C. 1995. Chlorophyll fluorescence as a nonintrusive
629 indicator for rapid assessment of in vivo photosynthesis. in: *Ecophysiology of*
630 *photosynthesis*, Springer, pp. 49-70.

631 Shao, J., Yu, G., Wu, Z., Peng, X., Li, R. 2010. Responses of Synechocystis sp. PCC 6803
632 (cyanobacterium) photosystem II to pyrene stress. *Journal of Environmental Sciences*,
633 **22**(7), 1091-1095.

634 Stauber, J.L., Franklin, N.M., Adams, M.S. 2002. Applications of flow cytometry to
635 ecotoxicity testing using microalgae. *Trends in Biotechnology*, **20**(4), 141-143.

636 Subashchandrabose, S.R., Krishnan, K., Gratton, E., Megharaj, M., Naidu, R. 2014. Potential
637 of Fluorescence Imaging Techniques To Monitor Mutagenic PAH Uptake by
638 Microalga. *Environmental Science & Technology*, **48**(16), 9152-9160.

639 Valavanidis, A., Vlachogianni, T., Triantafillaki, S., Dassenakis, M., Androutsos, F.,
640 Scoullos, M. 2008. Polycyclic aromatic hydrocarbons in surface seawater and in
641 indigenous mussels (Mytilus galloprovincialis) from coastal areas of the Saronikos
642 Gulf (Greece). *Estuarine, Coastal and Shelf Science*, **79**(4), 733-739.

643 Vecchiato, M., Turetta, C., Patti, B., Barbante, C., Piazza, R., Bonato, T., Gambaro, A. 2018.
644 Distribution of fragrances and PAHs in the surface seawater of the Sicily Channel,
645 Central Mediterranean. *Science of The Total Environment*, **634**, 983-989.

646 Vega-López, A., Ayala-López, G., Posadas-Espadas, B.P., Olivares-Rubio, H.F., Dzul-
647 Caamal, R. 2013. Relations of oxidative stress in freshwater phytoplankton with
648 heavy metals and polycyclic aromatic hydrocarbons. *Comparative Biochemistry and*
649 *Physiology Part A: Molecular & Integrative Physiology*, **165**(4), 498-507.

650 Villareal, T.A., Morton, S.L. 2002. Use of Cell-Specific PAM-Fluorometry to Characterize
651 Host Shading in the Epiphytic Dinoflagellate Gambierdiscus toxicus. *Marine*
652 *Ecology*, **23**(2), 127-140.

653 Vindimian, E. 2010. REGTOX: macro Excel™ for dose-response modelling.

654 Ya, M.-L., Wang, X.-H., Wu, Y.-L., Ye, C.-X., Li, Y.-Y. 2014. Enrichment and partitioning
655 of polycyclic aromatic hydrocarbons in the sea surface microlayer and subsurface
656 water along the coast of Xiamen Island, China. *Marine Pollution Bulletin*, **78**(1), 110-
657 117.

Yang, S., Wu, R.S.S., Kong, R.Y.C. 2002. Physiological and cytological responses of the marine diatom Skeletonema costatum to 2,4-dichlorophenol. *Aquatic Toxicology*, **60**(1), 33-41.

Zhang, H., Xue, M., Dai, Z. 2010. Determination of polycyclic aromatic hydrocarbons in aquatic products by HPLC-fluorescence. *Journal of Food Composition and Analysis*, **23**(5), 469-474.

Zhang, P., Liu, H., Yue, Z., Chen, B., Yao, M. 2015. Laser induced fluorescence spectroscopic analysis of aromatics from one ring to four rings. *Guang pu xue yu guang pu fen xi= Guang pu*, **35**(6), 1592-1596.

Zhou, J.L., Maskaoui, K. 2003. Distribution of polycyclic aromatic hydrocarbons in water and surface sediments from Daya Bay, China. *Environmental Pollution*, **121**(2), 269-281.